Eur. Phys. J. Plus (2015) **130**: 115
DOI 10.1140/epjp/i2015-15115-4

THE EUROPEAN PHYSICAL JOURNAL PLUS

Regular Article

Ferrofluid heat transfer treatment in the presence of variable magnetic field

M. Sheikholeslami[1,a] and M.M. Rashidi[2,3]

[1] Department of Mechanical Engineering, Babol University of Technology, Babol, Islamic Republic of Iran
[2] Shanghai Key Lab of Vehicle Aerodynamics and Vehicle Thermal Management Systems, Tongji University, Address: 4800 Cao An Rd., Jiading, Shanghai 201804, China
[3] ENN-Tongji Clean Energy Institute of Advanced Studies, Shanghai, China

Received: 3 January 2015 / Revised: 16 April 2015
Published online: 22 June 2015 –

Abstract. In this paper, the Control Volume-based Finite Element Method (CVFEM) is applied to simulate Fe_3O_4-water nanofluid mixed convection heat transfer in a lid-driven semi annulus in the presence of a non-uniform magnetic field. The calculations were performed for different governing parameters, namely, Richardson number, viscosity parameter, nanoparticle volume fraction, magnetic number and Hartmann number. Results show that the Nusselt number has a direct relationship with Richardson number and nanoparticle volume fraction, while it has a reverse relationship with Hartmann number and magnetic number. Also, it can be found that the Nusselt number increases by considering magnetic-field–dependent viscosity.

Nomenclature

B	Magnetic induction ($=\mu_0 H$) [T]	**Greek symbols**	
C_p	Specific heat at constant pressure [J/KgK]	ζ	Angle measured from the lower right plane
Ec	Eckert number ($=(\mu_f\alpha_f)/[(\rho C_P)_f \Delta T\, L^2]$)	α	Thermal diffusivity [m^2/s]
Gr_f	Grashof number	ϕ	Volume fraction
H_x, H_y	Components of the magnetic field intensity	γ'	Magnetic field strength at the source
H	The magnetic field strength [T]	ε_1	Temperature number ($=T_1/\Delta T$)
Ha	Hartmann number ($=\mu_0 H_0 L\sqrt{\sigma_f/\mu_f}$)	σ	Electrical conductivity [$(\Omega\cdot m)^{-1}$]
Mn_F	Magnetic number arising from FHD ($=\mu_0 H_0^2 K'(T_h-T_c)/(\rho_f U_{\rm lid}^2)$)	μ	Dynamic viscosity [kg/ms]
M	Magnetization ($=K'\overline{H}(T_c'-T)$)	μ_0	Magnetic permeability of vacuum ($=4\pi\times10^{-7} Tm/A$)
$Nu_{\rm loc}$	Local Nusselt number	υ	Kinematic viscosity [m^2/s]
$Nu_{\rm ave}$	Average Nusselt number	ψ and Ψ	Stream function and dimensionless stream function
Pr	Prandtl number ($=\upsilon_f/\alpha_f$)	Θ	Dimensionless temperature
T	Fluid temperature [K]	ρ	Fluid density [Kg/m^3]
T_c'	Curie temperature [K]	β	Thermal expansion coefficient [1/K]

[a] e-mail: m.sheikholeslami@mit.ac.ir

u, v	Velocity components in the x-direction and y-direction [m/s]	**Subscripts**	
U, V	Dimensionless velocity components in the X-direction and Y-direction [m/s]	c	Cold
x, y	Space coordinates [m]	h	Hot
X, Y	Dimensionless space coordinates [m]	ave	Average
r	Non-dimensional radial distance [m]	nf	Nanofluid
k	Thermal conductivity [W/m · k]	f	Base fluid
L	Gap between inner and outer boundary of the enclosure $L = r_{\text{out}} - r_{\text{in}} = r_{\text{in}}$	s	Solid particles
$\vec{g}$	Gravitational acceleration vector [m/s^2]	in	Inner
Ri	Richardson number ($= Gr/\text{Re}^2$)	out	Outer

1 Introduction

It is important to investigate the effect of a magnetic field on fluids, due to its uncountable applications in a wide spectrum of fields. The interaction of the magnetic field or the electromagnetic field with fluids has been studied, *e.g.*, among nuclear fusion, chemical engineering, medicine, high-speed noiseless printing and transformer cooling. Entropy analysis in an unsteady magnetohydrodynamic nanofluid regime adjacent to an accelerating stretching permeable surface with water as the base fluid and different types of nanoparticles was studied by Abolbashari *et al.* [1]. They found that this model has important applications in heat transfer enhancement in renewable energy systems, industrial thermal management and also materials processing. Mixed convective heat transfer of a water/alumina nanofluid inside a vertical microchannel was investigated by Malvandi and Ganji [2]. They showed that increasing the bulk mean volume fraction of nanoparticles, the slip parameter and the mixed convective parameter enhances the heat transfer rate. The influence of thermal radiation and heat generation on an unsteady two-dimensional natural convection flow in an inclined enclosure has been studied by Mahapatra *et al.* [3]. Their results indicated that the magnetic field suppresses the convection flow and its direction influences the flow pattern, which results in the appearance of inner loop and multiple eddies. Mahmoudi *et al.* [4] investigated the entropy generation and enhancement of heat transfer in natural convection flow and heat transfer using copper (Cu)-water nanofluid in the presence of a constant magnetic field. They observed that the entropy generation decreases when the nanoparticles are present, while the magnetic field generally increases the magnitude of the entropy generation. The problem of steady two-dimensional magnetohydrodynamic (MHD) stagnation-point flow and heat transfer, with thermal radiation, of a nanofluid past a shrinking sheet was investigated by Nandy and Pop [5]. They concluded that the Nusselt number and the Sherwood number are strongly influenced by the magnetic parameter. The effects of using different geometrical parameters with the combination of a nanofluid on heat transfer and fluid flow characteristics in a helically coiled tube heat exchanger (HCTHE) were numerically investigated by Mohammed and Narrein [6]. They found that the counter-flow configuration produced better results as compared to the parallel-flow configuration. Azizian *et al.* [7] studied the effect of an external magnetic field on the convective heat transfer and pressure drop of magnetite nanofluids under laminar flow regime conditions. They showed that the mechanisms for heat transfer enhancement are postulated to be an accumulation of particles near the magnets.

Numerical analysis of the heat transfer enhancement and fluid flow characteristics of a rotating cylinder under the influence of magnetic dipole in the backward facing step geometry was conducted by Selimefendigil and Oztop [8]. They found that the effect of the cylinder rotation on the local Nusselt number distribution is more pronounced at a low Reynolds number. Sheikholeslami Kandelousi [9] studied the effect of a spatially variable magnetic field on ferrofluid flow and heat transfer considering constant heat flux boundary condition. He found that enhancement in the heat transfer decreases with an increase in the Rayleigh number and the magnetic number but it increases with an increase in the Hartmann number. Nanjundappa *et al.* [10] studied the effect of magnetic-field–dependent (MFD) viscosity on the onset of ferro convection in a ferrofluid saturated horizontal porous layer. Free convection of ferrofluid in a cavity heated from below in the presence of an external magnetic field was studied by Sheikholeslami and Gorji [11]. They found that particles with a smaller size have a better ability to dissipate heat, and a larger volume fraction would provide a stronger driving force which leads to an increase in the temperature profile. Sheikholeslami and Rashidi [12] studied the effect of a space-dependent magnetic field on free convection of nanofluid. They showed that the Nusselt number decreases with an increase in Lorentz forces. MHD mixed convection of Cu-water nanofluid filled triangular enclosure with a rotating cylinder was investigated numerically by Selimefendigil and Oztop [13]. They found that heat transfer and total entropy generation increase as the solid volume fraction of nanoparticle increases. Hatami *et al.* [14] simulated the flow and heat transfer of a nanofluid flow between two parallel plates. They showed that in order

to reach the maximum Nusselt number, copper should be used as nanoparticle. Effects of the magnetic field on flow and heat transfer were considered by different authors [15–72].

The Control Volume-based Finite Element Method (CVFEM) uses the advantages of both the finite volume and finite element methods for the simulation of multi-physics problems in complex geometries [73]. Soleimani *et al.* [74] studied natural convection heat transfer in a semi-annulus enclosure filled with a nanofluid using the CVFEM. They found that the angle of turn has an important effect on the streamlines, isotherms and maximum or minimum values of the local Nusselt number. Ferrohydrodynamic and magnetohydrodynamic effects on ferrofluid flow and convective heat transfer were studied by Sheikholeslami and Ganji [75]. They proved that the magnetic number has a different effect on the Nusselt number corresponding to the Rayleigh number. Sheikholeslami *et al.* [76] studied the problem of natural convection between a circular enclosure and a sinusoidal cylinder. They concluded that streamlines, isotherms, and the number, size and formation of the cells inside the enclosure strongly depend on the Rayleigh number, values of amplitude and the number of undulations of the enclosure. This method was applied for various applications [77–85].

The main purpose of the present work is to study the mixed convection heat transfer of the ferrofluid in the presence of a non-uniform magnetic field. The CVFEM is applied to solve this problem. The numerical investigation is carried out for different governing parameters such as the Richardson number, viscosity parameter, nanoparticle volume fraction, magnetic number arising from FHD and Hartmann number arising from MHD.

2 Geometry definition and boundary conditions

The schematic diagram and the mesh of the semi-annulus enclosure used in the present CVFEM program are shown in fig. 1. The inner wall is maintained at constant temperatures T_h and the other walls are maintained at constant temperature $T_c (T_h > T_c)$. For the expression of the magnetic field strength it can be considered that the magnetic source represents a magnetic wire placed vertically to the x-y plane at the point $(\overline{a}, \overline{b})$. The components of the magnetic field intensity $(\overline{H_x}, \overline{H_y})$ and the magnetic field strength $(\overline{H})$ can be considered as [86]

$$\overline{H_x} = \frac{\gamma'}{2\pi} \frac{1}{(x-\overline{a})^2 + (y-\overline{b})^2} (y-\overline{b}) \tag{1}$$

$$\overline{H_y} = -\frac{\gamma'}{2\pi} \frac{1}{(x-\overline{a})^2 + (y-\overline{b})^2} (x-\overline{a}) \tag{2}$$

$$\overline{H} = \sqrt{\overline{H}_x^2 + \overline{H}_y^2} = \frac{\gamma'}{2\pi} \frac{1}{\sqrt{(x-\overline{a})^2 + (y-\overline{b})^2}}, \tag{3}$$

where γ' is the magnetic field strength at the source (of the wire) and $(\overline{a}, \overline{b})$ is the position where the source is located. The contours of the magnetic field strength are shown in fig. 2. In this study the magnetic source is located at (−0.01 cols, 0.5 rows). The upper wall is lid-driven with velocity of U_{lid}. In this study γ is equal to 45°.

3 Mathematical modeling and numerical procedure

3.1 Problem formulation

The flow is two-dimensional, laminar and incompressible. The magnetic Reynolds number is assumed to be small so that the induced magnetic field can be neglected compared to the applied magnetic field. The flow is considered to be steady, two-dimensional and laminar. Using the Boussinesq approximation, the governing equations of heat transfer and fluid flow for nanofluid can be obtained as follows:

$$\frac{\partial u}{\partial x} + \frac{\partial v}{\partial y} = 0 \tag{4}$$

$$\rho_{nf}\left(u\frac{\partial u}{\partial x} + v\frac{\partial u}{\partial y}\right) = -\frac{\partial P}{\partial x} + \eta\left(\frac{\partial^2 u}{\partial x^2} + \frac{\partial^2 u}{\partial y^2}\right) + \mu_0 M\frac{\partial \overline{H}}{\partial x} - \sigma_{nf}B_y^2 u + \sigma_{nf}B_x B_y v \tag{5}$$

$$\rho_{nf}\left(u\frac{\partial v}{\partial x} + v\frac{\partial v}{\partial y}\right) = -\frac{\partial P}{\partial y} + \eta\left(\frac{\partial^2 v}{\partial x^2} + \frac{\partial^2 v}{\partial y^2}\right) + \mu_0 M\frac{\partial \overline{H}}{\partial y} - \sigma_{nf}B_x^2 v + \sigma_{nf}B_x B_y u + \rho_{nf}\beta_{nf} g(T - T_c) \tag{6}$$

$$\begin{aligned}(\rho C_p)_{nf}\left(u\frac{\partial T}{\partial x} + v\frac{\partial T}{\partial y}\right) &= k_{nf}\left(\frac{\partial^2 T}{\partial x^2} + \frac{\partial^2 T}{\partial y^2}\right) + \sigma_{nf}(uB_y - vB_x)^2 - \mu_0 T\frac{\partial M}{\partial T}\left(u\frac{\partial \overline{H}}{\partial x} + v\frac{\partial \overline{H}}{\partial y}\right) \\ &\quad + \eta\left\{2\left(\frac{\partial u}{\partial x}\right)^2 + 2\left(\frac{\partial v}{\partial x}\right)^2 + \left(\frac{\partial u}{\partial x} + \frac{\partial v}{\partial y}\right)^2\right\},\end{aligned} \tag{7}$$

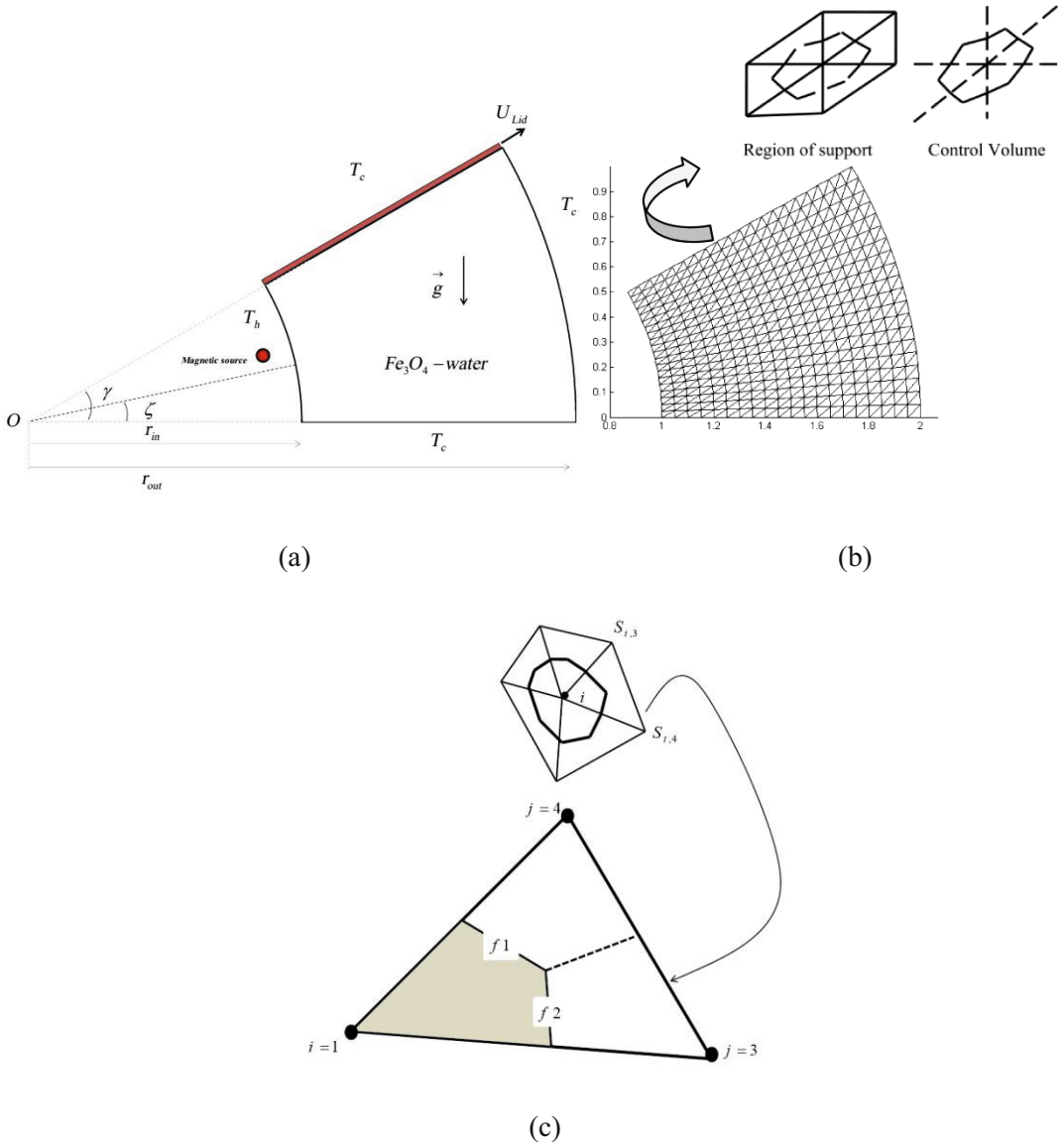

Fig. 1. (a) Geometry and the boundary conditions. (b) The mesh of enclosure considered in this work. (c) A sample triangular element and its corresponding control volume.

where $\eta = (1+\vec{\delta}\cdot\vec{B})\mu_{nf}$, the variation of MFD viscosity (δ) has been taken to be isotropic, $\delta_1 = \delta_2 = \delta_3 = \delta$. The terms $\mu_0 M \frac{\partial \overline{H}}{\partial x}$ and $\mu_0 M \frac{\partial \overline{H}}{\partial y}$ in (5) and (6), respectively, represent the components of magnetic force, per unit volume, and depend on the existence of the magnetic gradient on the corresponding x and y directions. These two terms are well known from FHD, which is the so-called Kelvin force. The terms $-\sigma_{nf}B_y^2 u + \sigma_{nf}B_x B_y v$ and $-\sigma_{nf}B_x^2 v + \sigma_{nf}B_x B_y u$ appearing in (5) and (6), respectively, represent the Lorentz force per unit volume towards the x and y directions and arise due to the electrical conductivity of the fluid. These two terms are known in MHD. The principles of MHD and FHD are combined in the mathematical model presented in [86] and the above-mentioned terms arise together in the governing equations (5) and (6). The term $\mu_0 T \frac{\partial M}{\partial T}\left(u\frac{\partial \overline{H}}{\partial x} + v\frac{\partial \overline{H}}{\partial y}\right)$ in eq. (7) represents the thermal power per unit volume due to the magneto-caloric effect. Also the term $\sigma_{nf}(uB_y - vB_x)^2$ in (7) represents the Joule heating. For the variation of the magnetization M, with the magnetic field intensity $\overline{H}$ and temperature T, the following relation derived experimentally in [16] and also used in [86] is considered:

$$M = K'\overline{H}\,(T_c' - T)\,, \tag{8}$$

where K' is a constant and T_c' is the Curie temperature. In the above equations, μ_0 is the magnetic permeability of vacuum ($4\pi \times 10^{-7} Tm/A$), $\overline{H}$ is the magnetic field strength, $\overline{B}$ is the magnetic induction ($\overline{B} = \mu_0 \overline{H}$) and the bar

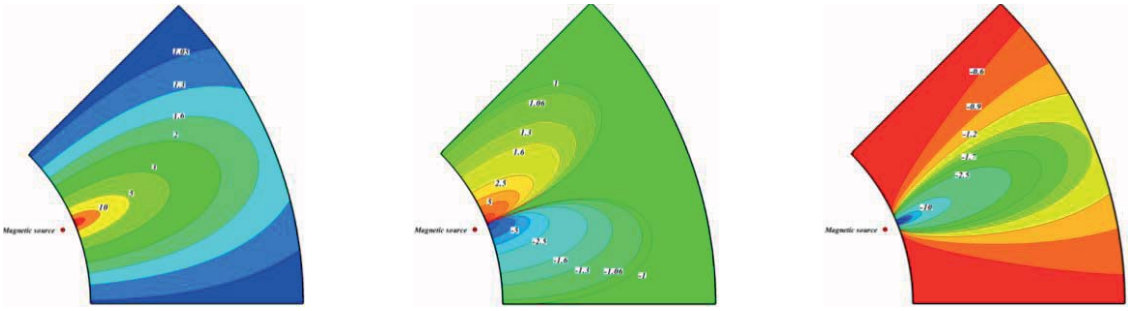

(a) $H(x,y)$ (b) $Hx(x,y)$ (c) $Hy(x,y)$

Fig. 2. Contours of the (a) magnetic field strength H; (b) magnetic field intensity component in the x-direction Hx; (c) magnetic field intensity component in the y-direction Hy.

above the quantities denotes that they are dimensional. The effective density (ρ_{nf}) and heat capacitance $(\rho C_p)_{nf}$ of the nanofluid are defined as [87]

$$\rho_{nf} = \rho_f(1-\phi) + \rho_s\phi \tag{9}$$

$$(\rho C_p)_{nf} = (\rho C_p)_f(1-\phi) + (\rho C_p)_s\phi, \tag{10}$$

where ϕ is the solid volume fraction of nanoparticles. Thermal diffusivity of the nanofluid is

$$\alpha_{nf} = k_{nf}/(\rho C_p)_{nf} \tag{11}$$

and the thermal expansion coefficient of the nanofluid can be determined as

$$\beta_{nf} = \beta_f(1-\phi) + \beta_s\phi. \tag{12}$$

The dynamic viscosity of the nanofluid given by Brinkman [87] is

$$\mu_{nf} = \mu_f(1-\phi)^{-2.5}. \tag{13}$$

The effective thermal conductivity of the nanofluid can be approximated by the Maxwell-Garnetts (MG) model as [87]

$$\frac{k_{nf}}{k_f} = \frac{k_s + 2k_f - 2\phi(k_f - k_s)}{k_s + 2k_f + \phi(k_f - k_s)} \tag{14}$$

and the effective electrical conductivity of nanofluid was presented by Maxwell [85] as below

$$\frac{\sigma_{nf}}{\sigma_f} = 1 + 3(\sigma_s/\sigma_f - 1)\phi/\left[(\sigma_s/\sigma_f + 2) - (\sigma_s/\sigma_f - 1)\phi\right]. \tag{15}$$

Let us introduce the following non-dimensional variables:

$$X = \frac{x}{L}, \qquad Y = \frac{y}{L}, \qquad \Theta = \frac{T - T_c}{T_h - T_c}, \qquad U = \frac{u}{U_{\text{lid}}},$$
$$V = \frac{v}{U_{\text{lid}}}, \qquad H = \frac{\overline{H}}{\overline{H_0}}, \qquad H_x = \frac{\overline{H_x}}{\overline{H_0}}, \qquad H_y = \frac{\overline{H_y}}{\overline{H_0}}, \tag{16}$$

where $\overline{H_0} = \overline{H}(\overline{a}, 0) = \frac{\gamma}{2\pi|b|}$ and $L = r_{\text{out}} - r_{\text{in}} = r_{\text{in}}$.

Table 1. Thermophysical properties of water and nanoparticles [87].

	ρ (kg/m^3)	C_p (j/kgk)	k (W/m $\cdot$ k)	$\beta \times 10^5$ (K^{-1})	d_p (nm)	σ $(\Omega \cdot \mathrm{m})^{-1}$
Pure water	997.1	4179	0.613	21	–	0.05
Fe_3O_4	5200	670	6	1.3	47	25000

Using the dimensionless parameters, the equations now become

$$\frac{\partial U}{\partial X}+\frac{\partial V}{\partial Y}=0 \tag{17}$$

$$U\frac{\partial U}{\partial X}+V\frac{\partial U}{\partial Y}=-\frac{\partial P}{\partial X}+\frac{1}{\mathrm{Re}}\left[\frac{\mu_{nf}/\mu_f}{\rho_{nf}/\rho_f}\right](1+\delta^*(H_x+H_y))\left(\frac{\partial^2 U}{\partial X^2}+\frac{\partial^2 U}{\partial Y^2}\right)$$
$$+Mn_F\left(\frac{\rho_f}{\rho_{nf}}\right)(\varepsilon_2-\varepsilon_1-\Theta)H\frac{\partial H}{\partial X}-\frac{Ha^2}{\mathrm{Re}}\left[\frac{\sigma_{nf}/\sigma_f}{\rho_{nf}/\rho_f}\right](H_y^2U-H_xH_yV) \tag{18}$$

$$U\frac{\partial V}{\partial X}+V\frac{\partial V}{\partial Y}=-\frac{\partial P}{\partial X}+\frac{1}{\mathrm{Re}}\left[\frac{\mu_{nf}/\mu_f}{\rho_{nf}/\rho_f}\right](1+\delta^*(H_x+H_y))\left(\frac{\partial^2 V}{\partial X^2}+\frac{\partial^2 V}{\partial Y^2}\right)$$
$$+Mn_F\left(\frac{\rho_f}{\rho_{nf}}\right)(\varepsilon_2-\varepsilon_1-\Theta)H\frac{\partial H}{\partial Y}-\frac{Ha^2}{\mathrm{Re}}\left[\frac{\sigma_{nf}/\sigma_f}{\rho_{nf}/\rho_f}\right](H_x^2V-H_xH_yU)+\frac{Gr}{\mathrm{Re}^2}\left[\frac{\beta_{nf}}{\beta_f}\right]\Theta \tag{19}$$

$$U\frac{\partial \Theta}{\partial X}+V\frac{\partial \Theta}{\partial Y}=\frac{1}{\mathrm{Pr}\,\mathrm{Re}}\left[\frac{\frac{k_{nf}}{k_f}}{\frac{(\rho C_P)_{nf}}{(\rho C_P)_f}}\right]\left(\frac{\partial^2\Theta}{\partial X^2}+\frac{\partial^2\Theta}{\partial Y^2}\right)+Ha^2\,\frac{Ec}{\mathrm{Re}}\left[\frac{\frac{\sigma_{nf}}{\sigma_f}}{\frac{(\rho C_P)_{nf}}{(\rho C_P)_f}}\right]\{U\,H_y-V\,H_x\}^2$$
$$+Mn_FEc\frac{(\rho C_P)_f}{(\rho C_P)_{nf}}\left\{U\frac{\partial H}{\partial X}+V\frac{\partial H}{\partial Y}\right\}H(\varepsilon_1+\Theta)$$
$$+\frac{Ec}{\mathrm{Re}}\left[\frac{\frac{\mu_{nf}}{\mu_f}}{\frac{(\rho C_P)_{nf}}{(\rho C_P)_f}}\right](1+\delta^*(H_x+H_y))\left\{2\left(\frac{\partial U}{\partial X}\right)^2+2\left(\frac{\partial V}{\partial Y}\right)^2+\left(\frac{\partial U}{\partial Y}+\frac{\partial V}{\partial X}\right)^2\right\}, \tag{20}$$

where $\mathrm{Re}=\frac{\rho_f L\,U_{\mathrm{lid}}}{\mu_f}$, $Gr=g\beta\Delta TL^3/\upsilon^2$, $Ha=LH_0\mu_0\sqrt{\sigma_f/\mu_f}$, $\varepsilon_1=T_1/\Delta T$, $Ec=(\rho_fU_{\mathrm{lid}}^2)/[(\rho C_P)_f\Delta T]$, $Ri=Gr/\mathrm{Re}^2$, $\delta^*=\delta\mu_0H_0$ and $Mn_F=\mu_0H_0^2K'(T_h-T_c)/(\rho_f\,U_{\mathrm{lid}}^2)$ are the Reynolds number, Grashof number, Hartmann number arising from MHD, temperature number, Eckert number, Richardson number, viscosity parameter and Magnetic number arising from FHD the for the base fluid, respectively. The thermophysical properties of the nanofluid are given in table 1 [88].

The stream function and vorticity are defined as

$$u=\frac{\partial\psi}{\partial y}\,,\qquad v=-\frac{\partial\psi}{\partial x}\,,\qquad \omega=\frac{\partial v}{\partial x}-\frac{\partial u}{\partial y}$$
$$\Omega=\frac{\omega L}{U_{\mathrm{lid}}}\,,\qquad \Psi=\frac{\psi}{LU_{\mathrm{lid}}}\,. \tag{21}$$

The stream function satisfies the continuity equation (17). The vorticity equation is obtained by eliminating the pressure between the two momentum equations, *i.e.* by taking y-derivative of eq. (19) and subtracting from it the x-derivative of eq. (18).

The boundary conditions as shown in fig. 1 are

$$\Theta=1.0\quad\text{on the inner circular boundary,}$$
$$\Theta=0.0\quad\text{on the other walls.} \tag{22}$$

The values of vorticity on the boundary of the enclosure can be obtained using the stream function formulation and the known velocity conditions during the iterative solution procedure.

The local Nusselt number of the nanofluid along the hot wall can be expressed as

$$Nu_{\mathrm{loc}}=\left(\frac{k_{nf}}{k_f}\right)\frac{\partial\Theta}{\partial r}\,, \tag{23}$$

where r is the radial direction. The average Nusselt number on the hot circular wall is evaluated as

$$Nu_{\mathrm{ave}}=\frac{1}{\gamma}\int_0^{\gamma}Nu_{\mathrm{loc}}(\zeta)\mathrm{d}\zeta. \tag{24}$$

Table 2. Comparison of the average Nusselt number Nu_{ave} along hot wall for different grid resolution at $Ri = 10$, Re $= 100$, $\phi = 0.04$, $Mn_F = 10$, $Ha = 10$, $Ec = 10^{-5}$, $\varepsilon_1 = 0$, δ^* and Pr $= 6.8$.

51×151	61×181	71×211	81×241	91×271	101×301
5.532671	5.532578	5.54671	5.556102	5.557318	5.558602

Table 3. Comparison of the present results with previous works for different Rayleigh numbers when Pr $= 0.7$.

Ra	Present	Khanafer *et al.* [88]	De Vahl Davis [89]
10^3	1.1432	1.118	1.118
10^4	2.2749	2.245	2.243
10^5	4.5199	4.522	4.519

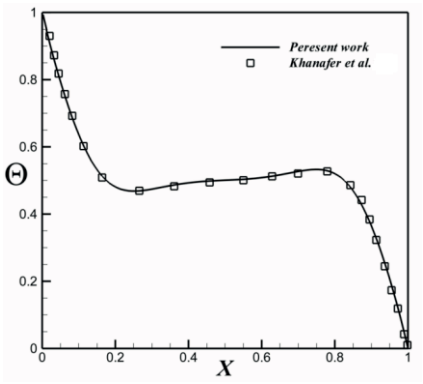

Fig. 3. Comparison of the average Nusselt number between the present results and numerical results by Khanafer *et al.* [88] $Gr = 10^4$, $\phi = 0.1$ and Pr $= 6.8$ (Cu-Water).

3.2 Numerical procedure

A control volume finite element method is used in this work. The building block of the discretization is the triangular element and the values of variables are approximated with linear interpolation within the elements. The control volumes are created by joining the center of each element in the support to the mid points of the element sides that pass through the central node i which creates a close polygonal control volume (see fig. 1(c)). The set of governing equations is integrated over the control volume with the use of linear interpolation inside the finite element and the obtained algebretic equations are solved by the Gauss-Seidel method. A FORTRAN code is developed to solve the present problem using a structured mesh of linear triangular. The details of this method are mentioned in [73].

4 Grid testing and code validation

A mesh testing procedure was conducted to guarantee the grid independency of the present solution. Various mesh combinations were explored for the case of $Ri = 10$, Re $= 100$, $\phi = 0.04$, $Mn_F = 10$, $Ha = 10$, $Ec = 10^{-5}$, $\varepsilon_1 = 0$, $\delta^* = 0$, and Pr $= 6.8$ as shown in table 2. The present code was tested for grid independence by calculating the average Nusselt number on the inner hot wall. In harmony with this, it was found that a grid size of 81×241 ensures a grid-independent solution. The convergence criterion for the termination of all computations is

$$\max_{grid} \left| \Gamma^{n+1} - \Gamma^{n} \right| \leq 10^{-7}, \tag{25}$$

where n is the iteration number and Γ stands for the independent variables (Ω, Ψ, Θ). To validate the present study the results obtained using the CVFEM code are compared for Pr $= 0.7$ with other works reported in [88] and [89] as seen in table 3. Moreover, the code was tested with the work of Khanafer *et al.* [88] in fig. 3 for natural convection in an enclosure filled with Cu-water nanofluid. These comparisons illustrate an excellent agreement between the present calculations and the previous works.

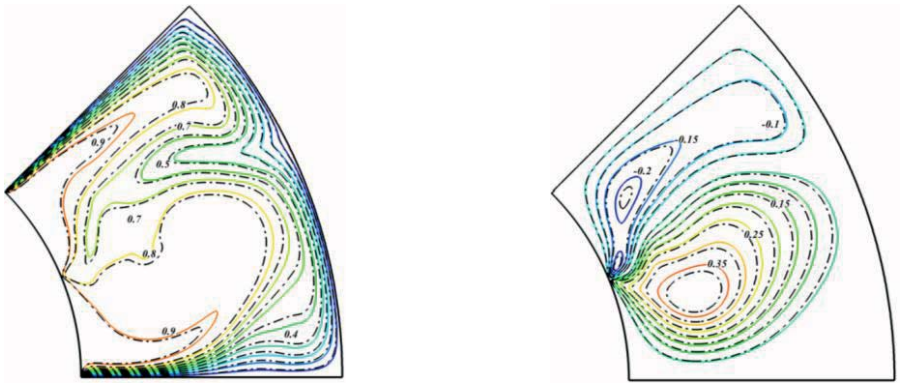

Fig. 4. Comparison of the streamlines between nanofluid ($\phi = 0.04$) ($- \cdot - \cdot -$) and pure fluid ($\phi = 0$) (—) when $Ri = 10$, Re $= 100$, $Mn_F = 10$, $Ha = 10$, $Ec = 10^{-5}$, $\varepsilon_1 = 0$, $\delta^* = 0$, Pr $= 6.8$.

5 Results and discussion

In this study, mixed convection heat transfer of ferrofluid in presence of variable magnetic field is investigated using CVFEM. Also the effect of magnetic field dependent (MFD) viscosity on hydrothermal behavior is considered. The mathematical model used for the formulation of the problem is consistent with the principles of FHD and MHD. The thermophysical properties of Fe_3O_4 nanoparticles and based fluid (water) are shown in table 1 [87]. Calculations are made for various values of volume fraction of nanoparticles ($\phi = 0\%$ and 4%), Richardson numbers ($Ri = 0.001$, 1 and 10), magnetic number ($Mn_F = 0$, 2, 4, 6 and 10), Hartmann number ($Ha = 0$, 5 and 10) and viscosity parameter ($\delta^* = 0$, 0.2, 0.4 and 0.6). In all calculations, the Prandtl number (Pr), temperature number (ε_1), Eckert number (Ec) and Reynolds number (Re) are set to 6.8, 0.0, 10^{-5} and 100, respectively.

Comparison of the streamlines between nanofluid and pure fluid is shown in fig. 4. The velocity components of nanofluid are increased because of an increase in the energy transport in the fluid with the increasing of volume fraction. Thermal boundary layer thickness decreases with increase of nanofluid volume fraction. Isotherms and streamlines contours for different values of viscosity parameter, Richardson, Hartmann and magnetic numbers are shown in figs. 5, 6 and 7. When $Ri = 0.01$, the heat transfer in the enclosure is mainly dominated by the conduction mode. At $Mn_F = 0$, $Ha = 0$ the streamlines show one rotating eddy. When Hartmann number increases a small vortex generates near the magnetic source, so thermal plume appears in this region. As magnetic number increases, the main vortex turns in to two smaller vortexes and in turn reverse thermal plume appears near the location of magnetic source. As Richardson number increases, the role of convection in heat transfer becomes more significant. At $Ri = 10$, the center of main vortex move downward and thermal boundary layer thickness near the inner wall becomes thinner. When Hartmann and magnetic numbers increase up to 10, the main vortex turns in to three eddies. Three thermal plumes generate over the inner wall due to existence of eddies which are rotated in different direction. Also, it can be seen that as viscosity parameter increases thermal boundary layer thickness decreases and one counter clock wise eddy generates at center of the enclosure.

Figure 8 depicts that the effects of magnetic number, Hartmann number, viscosity parameter and Richardson number on average Nusselt number. Thermal boundary layer thickness increases with increase of magnetic number, Hartmann number while it decreases with augment of Richardson number. So, average Nusselt number increases with increase of Richardson number while it decreases with increase of Hartmann number and magnetic number. Also it can be concluded that by considering the effect of magnetic field on viscosity of the fluid, rate of heat transfer increases.

6 Conclusions

In this study, mixed convection heat transfer in a lid driven semi annulus enclosure filled with Fe_3O_4-water nanofluid is investigated in presence of external magnetic field. Effect of magnetic field on viscosity is taken into account. The CVFEM is used to solve the governing equations. The effects of Richardson number, nanoparticle volume fraction, viscosity parameter, magnetic number and Hartmann number on the flow and heat transfer characteristics have been examined. The results show that increasing Richardson number and nanoparticle volume fraction lead to augmentation of the Nusselt number but Nusselt number decreases with increase of Hartmann number and magnetic number. Also, considering magnetic field dependent viscosity can enhance the rate of heat transfer. Moreover, the heat transfer enhancement decreases with increase of magnetic number while it increases with increase of Hartmann number and Richardson number.

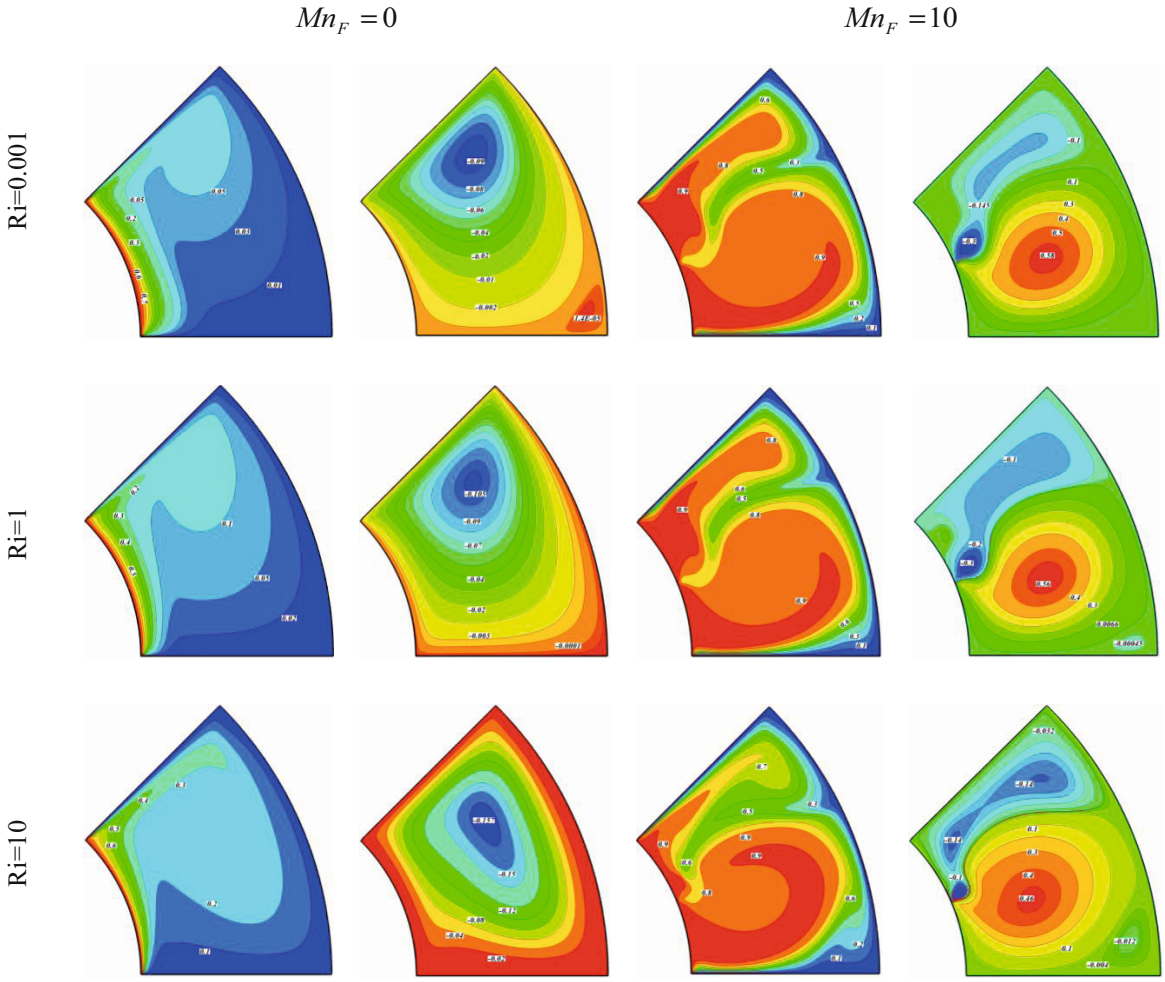

Fig. 5. Isotherms (left) and streamlines (right) contours for different values of Richardson number and magnetic number when $Ha = 0$, $\delta^* = 0$.

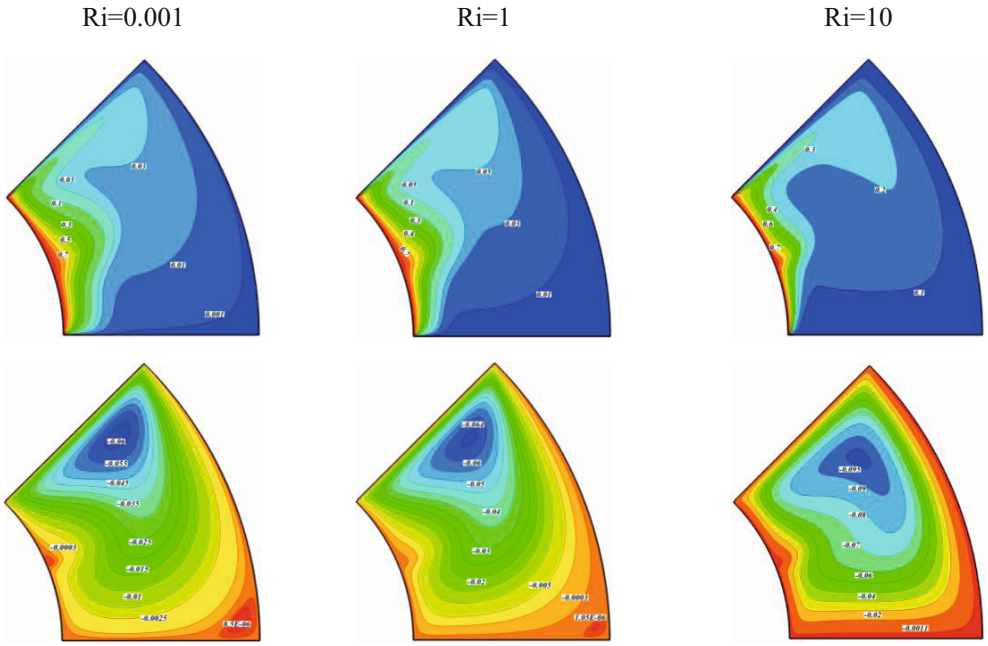

Fig. 6. Isotherms (top) and streamlines (bottom) contours for different values of the Richardson number when $Mn_F = 0$, $Ha = 10$, $\delta^* = 0$.

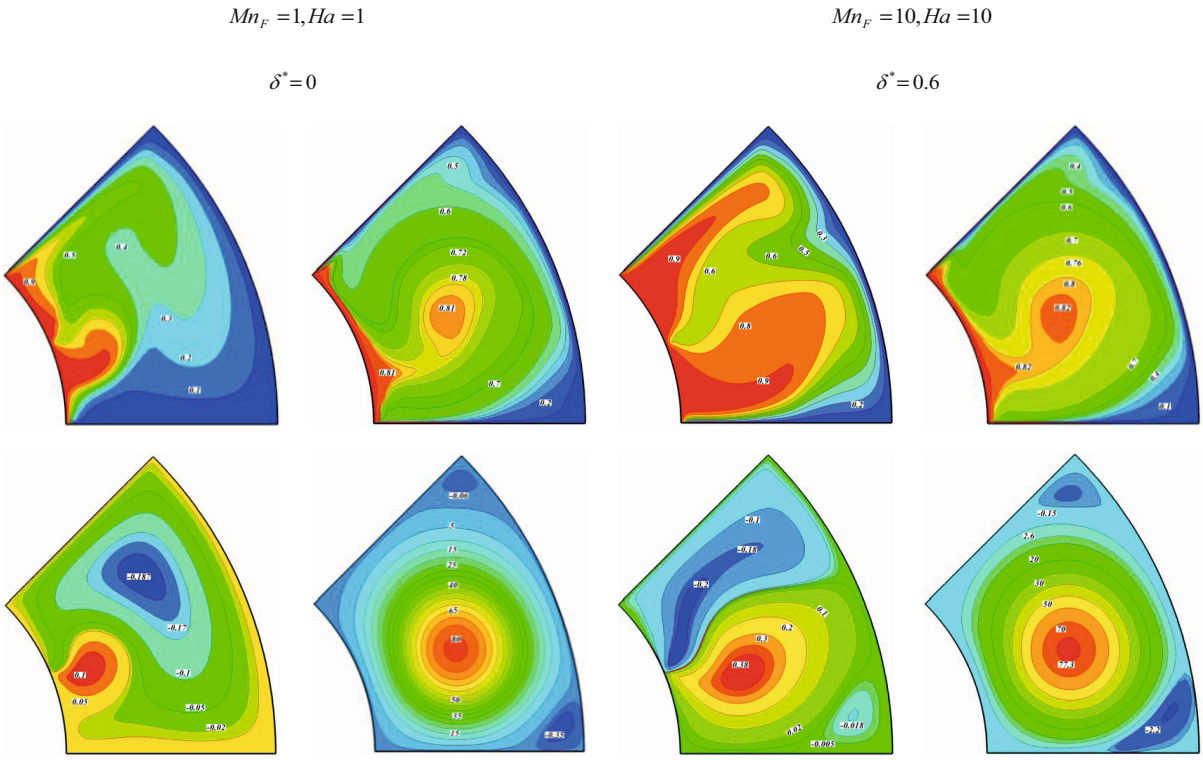

Fig. 7. Isotherms (left) and streamlines (right) contours for different values of δ^*, Ha and Mn_F when $Ri = 10$.

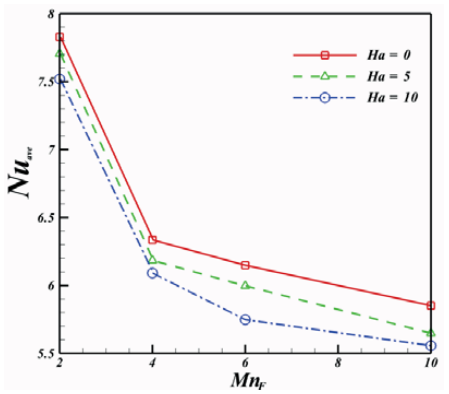

$Ri = 10$

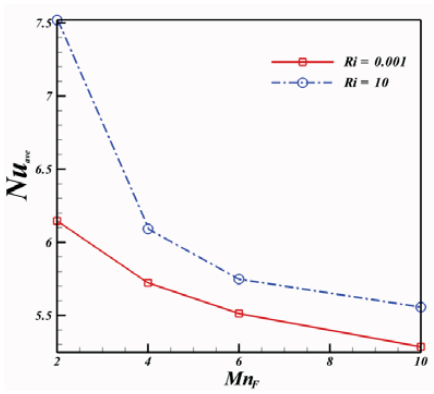

$Ha = 10$

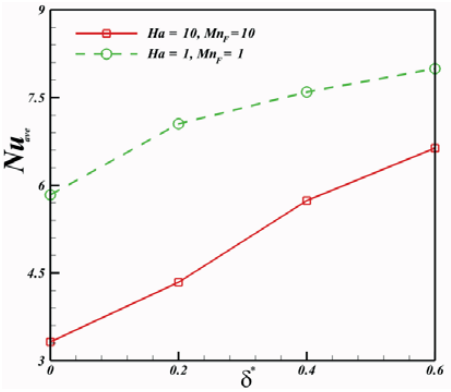

$Ri = 10$

Fig. 8. Effects of Ha, Mn_F, Ri and δ^* on the average Nusselt number Nu_{ave} along hot wall.

References

1. Mohammad Hossein Abolbashari, Navid Freidoonimehr, Foad Nazaria, Mohammad Mehdi Rashidi, Powder Technol. **267**, 256 (2014).
2. A. Malvandi, D.D. Ganji, Powder Technol. **263**, 37 (2014).
3. Tapas Ray Mahapatra, Dulal Pal, Sabyasachi Mondal, Int. Commun. Heat Mass Transfer **41**, 47 (2013).
4. Amir Houshang Mahmoudi, Ioan Pop, Mina Shahia, Farhad Talebi, Comp. Fluids **72**, 46 (2013).
5. Samir Kumar Nandy, Ioan Pop, Int. Commun. Heat Mass Transfer **53**, 50 (2014).
6. H.A. Mohammed, K. Narrein, Int. Commun. Heat Mass Transfer **39**, 1375 (2012).
7. R. Azizian, E. Doroodchi, T. McKrell, J. Buongiorno, L.W. Hu, B. Moghtaderi, Int. J. Heat Mass Transfer **68**, 94 (2014).
8. Fatih Selimefendigil, Hakan F. Oztop, Int. J. Heat Mass Transfer **71**, 142 (2014).
9. Mohsen Sheikholeslami Kandelousi, Eur. Phys. J. Plus **129**, 248 (2014).
10. C.E. Nanjundappa, I.S. Shivakumara, M. Ravisha, Int. Commun. Heat Mass Transfer **37**, 1246 (2010).
11. Mohsen Sheikholeslami, Mofid Gorji-Bandpy, Powder Technol. **256**, 490 (2014).
12. Mohsen Sheikholeslami, Mohammad Mehdi Rashidi, J. Taiwan Inst. Chem. Eng., doi:10.1016/j.jtice.2015.03.035 (2015).
13. Fatih Selimefendigil, Hakan F. Oztop, J. Taiwan Inst. Chem. Eng. **45**, 2150 (2014).
14. M. Hatami, M. Sheikholeslami, D.D. Ganji, J. Mol. Liq. **195**, 230 (2014).
15. Fatih Selimefendigil, Hakan F. Oztop, Int. J. Thermal Sci. **86**, 258 (2014).
16. Mohsen Sheikholeslami, Shirley Abelman, IEEE Trans. Nanotechnol. **14**, 561 (2015) doi:10.1109/TNANO.2015.2416318.
17. Mohsen Sheikholeslami, Mofid Gorji Bandpy, Hamid Reza Ashorynejad, Phys. A: Stat. Mech. Appl. **432**, 58 (2015).
18. Mohsen Sheikholeslami, Davood Domiri Ganji, Comput. Methods Appl. Mech. Eng. **283**, 651 (2015).
19. Mohsen Sheikholeslami, M.T. Mustafa, Particuology, doi:10.1016/j.partic.2014.09.004 (2015).
20. Fatih Selimefendigil, Hakan F. Öztop, Int. J. Heat Mass Transfer **71**, 142 (2014).
21. Fatih Selimefendigil, Hakan F. Öztop, Khaled Al-Salem, J. Magn. & Magn. Mater. **372**, 122 (2014).
22. M. Sheikholeslami, R. Ellahi, J. Z. Naturforsch. **70**, 115 (2015).
23. M. Sheikholeslami, M. Hatami, G. Domairry, J. Taiwan Inst. Chem. Eng. **46**, 43 (2015).
24. Mohsen Sheikholeslami Kandelousi, Phys. Lett. A **378**, 3331 (2014).
25. Mohsen Sheikholeslami, Davood Domiri Ganji, Phys. A **417**, 273 (2015).
26. Mohsen Sheikholeslami, Mofid Gorji-Bandpy, Kuppalapalle Vajravelu, Int. J. Heat Mass Transfer **80**, 16 (2015).
27. M. Sheikholeslami, J. Braz. Soc. Mech. Sci. Eng., doi:10.1007/s40430-014-0242-z (2014).
28. M. Mustafa, S. Hina, T. Hayat, A. Alsaedi, Int. J. Heat Mass Transfer **55**, 4871 (2012).
29. M. Mustafaa, T. Hayat, I. Pop, S. Asghare, S. Obaidat, Int. J. Heat Mass Transfer **54**, 5588 (2011).
30. Mohsen Sheikholeslami, Davood Domiri Ganji, M. Younus Javed, R. Ellahi, J. Magn. & Magn. Mater. **374**, 36 (2015).
31. Mohsen Sheikholeslami, Shirley Abelman, Davood Domiri Ganji, Int. J. Heat Mass Transfer **79**, 212 (2014).
32. Mohsen Sheikholeslami, Davood Domiri Ganji, J. Braz. Soc. Mech. Sci. Eng. **37**, 895 (2014).
33. M. Sheikholeslami, M. Gorji-Bandpay, D.D. Ganji, Arab. J. Sci. Eng. **39**, 5007 (2014).
34. M. Sheikholeslami, D.D. Ganji, J. Appl. Fluid Mech. **7**, 535 (2014).
35. S. Nadeem, Rashid Mehmood, Noreen Sher Akbar, J. Comput. Theor. Nanosci. **10**, 2737 (2013).
36. Mohsen Sheikholeslami, M. Hatami, M. Jafaryar, F. Farkhadnia, Davood Domiri Ganji, Mofid Gorji-Bandpy, Energy Build. **88**, 361 (2015).
37. N.S. Akbar, S. Nadeem, R.U. Haq, Ul Rizwan, Z.H. Khan, J. Comput. Theor. Nanosci. **11**, 47 (2014).
38. S.A. Shehzad, M. Qasim, A. Alsaedi, T. Hayat, M.S. Alhuthali, Eur. Phys. J. Plus **128**, 7 (2013).
39. S.A. Shehzad, F.E. Alsaadi, S.J. Monaquel, T. Hayat, Eur. Phys. J. Plus **128**, 56 (2013).
40. Mohsen Sheikholeslami, Mofid Gorji-Bandpy, Davood Domiri Ganji, Renew. Sustain. Energy Rev. **49**, 444 (2015).
41. Mohsen Sheikholeslami, Mofid Gorji Bandpy, R. Ellahi, A. Zeeshan, J. Magn. & Magn. Mater. **369**, 69 (2014).
42. M. Sheikholeslami, M. Gorji-Bandpy, D.D. Ganji, Soheil Soleimani, Trans. Mech. Eng. **38**, 217 (2014).
43. M. Sheikholeslami, M. Gorji-Bandpy, D.D. Ganji, J. Taiwan Inst. Chem. Eng. **45**, 1204 (2014).
44. Mohammad Hatami, Mohsen Sheikholeslami, M. Hosseini, Davood Domiri Ganji, J. Mol. Liq. **194**, 251 (2014).
45. M. Hatami, D.D. Ganji, Particuology **16**, 206 (2014).
46. M. Hatami, D.D. Ganji, Powder Technol. **258**, 94 (2014).
47. M. Hatami, D.D. Ganji, Int. J. Refrig. **40**, 140 (2014).
48. M. Hatami, M. Sheikholeslami, D.D. Ganji, Powder Technol. **253**, 769 (2014).
49. M. Sheikholeslami, E. Ellahi, Int. J. Heat Mass Transfer **89**, 799 (2015).
50. M. Sheikholeslami, D.D. Ganji, Sci. Iran. B **21**, 203 (2014).
51. M. Sheikholeslami, D.D. Ganji, J. Mol. Liq. **194**, 13 (2014).
52. M. Sheikholeslami, M. Gorji-Bandpy, D.D. Ganji, Powder Technol. **254**, 82 (2014).
53. M. Sheikholeslami, D.D. Ganji, Powder Technol. **253**, 789 (2014).
54. M. Sheikholeslami, M. Hatami, D.D. Ganji, J. Mol. Liq. **190**, 112 (2014).
55. M. Sheikholeslami, M. Gorji-Bandpy, D.D. Ganji, Energy **60**, 501 (2013).
56. M. Sheikholeslami, M. Gorji Bandpy, R. Ellahi, Mohsan Hassan, Soheil Soleimani, J. Magn. & Magn. Mater. **349**, 188 (2014).
57. M. Sheikholeslami, F. Bani Sheykholeslami, S. Khoshhal, H. Mola-Abasi, D.D. Ganji, Houman B. Rokni, Neural. Comput. Appl. **25**, 171 (2014).

58. M. Sheikholeslami, M. Gorji-Bandpy, S.M. Seyyedi, D.D. Ganji, Houman B. Rokni, Soheil Soleimani, Powder Technol. **247**, 87 (2013).
59. M. Sheikholeslami, M. Gorji-Bandpy, D.D. Ganji, Sci. Iran., Trans. B: Mech. Eng. **20**, 1241 (2013).
60. M. Sheikholeslami, M. Hatami, D.D. Ganji, Powder Technol. **246**, 327 (2013).
61. M. Sheikholeslami, M. Gorji-Bandpy, G. Domairry, Appl. Math. Mech. **34**, 1 (2013).
62. M. Sheikholeslami, D.D. Ganji, H.R. Ashorynejad, Powder Technol. **239**, 259 (2013).
63. M. Sheikholeslami, D.D. Ganji, Powder Technol. **235**, 873 (2013).
64. H.R. Ashorynejad, M. Sheikholeslami, I. Pop, D.D. Ganji, Heat Mass Transfer **49**, 427 (2013).
65. Hamid Reza Ashorynejad, Abdulmajeed A. Mohamad, Mohsen Sheikholeslami, Int. J. Therm. Sci. **64**, 240 (2013).
66. M. Sheikholeslami, M. Gorji-Bandpy, D.D. Ganji, Soheil Soleimani, S.M. Seyyedi, Int. Commun. Heat Mass Transfer **39**, 1435 (2012).
67. M. Sheikholeslami, M. Gorji-Bandpay, D.D. Ganji, Int. Commun. Heat Mass Transfer **39**, 978 (2012).
68. M. Sheikholeslami, D.D. Ganji, H.R. Ashorynejad, Houman B. Rokni, Appl. Math. Mech. **33**, 1553 (2012).
69. Davood Domairry, Mohsen Sheikholeslami, Hamid Reza Ashorynejad, Rama Subba Reddy Gorla, Mostafa Khani, Proc. Inst. Mech. Eng. N: J. Nanoeng. Nanosyst. **225**, 115 (2011) doi:10.1177/1740349911433468.
70. M. Sheikholeslami, H.R. Ashorynejad, D.D. Ganji, A. Yıldırım, Sci. Iran. B **19**, 437 (2012).
71. M. Sheikholeslami, H.R. Ashorynejad, D.D. Ganji, A. Kolahdooz, Math. Probl. Eng. **2011**, 258734 (2011) doi:10.1155/2011/258734.
72. M. Sheikholeslami, D.D. Ganji, Houman B. Rokni, Int. J. Eng. Trans. **26**, 653 (2013).
73. Mohsen Sheikholeslami, Davood Domairry Ganji, *Hydrothermal Analysis in Engineering Using Control Volume Finite Element Method* (Academic Press, 2015) ISBN: 9780128029503.
74. Soheil Soleimani, M. Sheikholeslami, D.D. Ganji, M. Gorji-Bandpay, Int. Commun. Heat Mass Transfer **39**, 565 (2012).
75. M. Sheikholeslami, D.D. Ganji, Energy **75**, 400 (2014).
76. M. Sheikholeslami, M. Gorji-Bandpy, I. Pop, Soheil Soleimani, Int. J. Therm. Sci. **72**, 147 (2013).
77. Mohsen Sheikholeslami, Davood Domiri Ganji, Mohammad Mehdi Rashidi, J. Taiwan Inst. Chem. Eng. **47**, 6 (2015).
78. M. Sheikholeslami, M. Gorji-Bandpy, D.D. Ganji, P. Rana, Soheil Soleimani, Comp. Fluids **94**, 147 (2014).
79. M. Sheikholeslami, M. Gorji-Bandpy, D.D. Ganji, Soheil Soleimani, J. Mol. Liq. **194**, 179 (2014).
80. M. Sheikholeslami, M. Gorji-Bandpy, D.D. Ganji, Soheil Soleimani, J. Mol. Liq. **193**, 174 (2014).
81. M. Sheikholeslami, D.D. Ganji, M. Gorji-Bandpy, Soheil Soleimani, J. Taiwan Inst. Chem. Eng. **45**, 795 (2014).
82. M. Sheikholeslami, M. Gorji-Bandpy, Soheil Soleimani, Int. Commun. Heat Mass Transfer **47**, 73 (2013).
83. M. Sheikholeslami, M. Gorji-Bandpy, D.D. Ganji, Soheil Soleimani, J. Taiwan Inst. Chem. Eng. **45**, 40 (2014).
84. M. Sheikholeslami, M. Gorji-Bandpy, D.D. Ganji, Soheil Soleimani, Adv. Powder Technol. **24**, 980 (2013).
85. M. Sheikholeslami, M. Gorji-Bandpy, D.D. Ganji, Soheil Soleimani, Neural. Comput. Appl. **24**, 873 (2014).
86. V. Loukopoulos, E. Tzirtzilakis, Int. J. Eng. Sci. **42**, 571 (2004).
87. K. Khanafer, K. Vafai, M. Lightstone, Int. J. Heat Mass Transfer **46**, 3639 (2003).
88. H. Aminfar, M. Mohammadpourfard, F. Mohseni, J. Magn. & Magn. Mater. **324**, 830 (2012).
89. G. De Vahl Davis, Int. J. Numer. Methods Fluids **3**, 249 (1962).